Organelle Assembly in Yeast: Characterization of Yeast Mutants Defective in Vacuolar Biogenesis and Protein Sorting

Lois M. Banta, Jane S. Robinson, Daniel J. Klionsky, and Scott D. Emr

Division of Biology, 147-75, California Institute of Technology, Pasadena, California 91125

Abstract. Yeast vacuole protein targeting (*vpt*) mutants exhibit defects in the sorting and processing of multiple vacuolar hydrolases. To evaluate the impact these *vpt* mutations have on the biogenesis and functioning of the lysosome-like vacuole, we have used light and electron microscopic techniques to analyze the vacuolar morphology in the mutants. These observations have permitted us to assign the *vpt* mutants to three distinct classes. The class A *vpt* mutants (26 complementation groups) contain 1–3 large vacuoles that are morphologically indistinguishable from those in the parental strain, suggesting that only a subset of the proteins destined for delivery to this compartment is mislocalized. One class A mutant (*vpt*13) is very sensitive to low pH and exhibits a defect in vacuole acidification. Consistent with a potential role for vacuolar pH in protein sorting, we found that bafilomycin A_1, a specific inhibitor of the vacuolar ATPase, as well as the weak base ammonium acetate and the proton ionophore carbonyl cyanide *m*-chlorophenylhydrazone, collapse the pH gradient across the vacuolar membrane and cause the missorting and secretion of two vacuolar hydrolases in wild-type cells. Mutants in the three class B *vpt* complementation groups exhibit a fragmented vacuole morphology. In these mutants, no large normal vacuoles are observed. Instead, many (20–40) smaller vacuole-like organelles accumulate. The class C *vpt* mutants, which constitute four complementation groups, exhibit extreme defects in vacuole biogenesis. The mutants lack any organelle resembling a normal vacuole but accumulate other organelles including vesicles, multilamellar membrane structures, and Golgi-related structures. Heterozygous class C zygotes reassemble normal vacuoles rapidly, indicating that some of the accumulated aberrant structures may be intermediates in vacuole formation. These class C mutants also exhibit sensitivity to osmotic stress, suggesting an osmoregulatory role for the vacuole. The *vpt* mutants should provide insights into the normal physiological role of the vacuole, as well as allowing identification of components required for vacuole protein sorting and/or vacuole assembly.

EUKARYOTIC cells are distinguished by their several discrete membrane-enclosed organelles. Each of these subcellular compartments has unique structural and functional characteristics which are conferred in large part by the distinct set of proteins that constitute that organelle. Thus, accurate sorting and trafficking of proteins from their site of synthesis in the cytoplasm to their correct noncytoplasmic destinations are essential for maintaining the functional and structural identity of each organelle.

In mammalian cells, the secretory pathway has been shown to mediate the modification, processing, and delivery of proteins destined for a variety of intracellular and extracellular compartments. Proteins destined for secretion, assembly into the plasma membrane, delivery to lysosomes, or retention within endoplasmic reticulum (ER)[1] and Golgi compartments transit through all or a portion of the secretory pathway (11). Presently, available data are consistent with a model in which much of protein secretion occurs via a default mechanism (5). Proteins competent for entry into the ER but lacking any additional sorting information passively transit from the ER to the Golgi complex and then are secreted via a nonspecific bulk flow mechanism (58). However, proteins that depart from this pathway, such as lysosomal enzymes, contain additional sorting signals that permit specific recognition, modification, and subsequent delivery of these proteins from late Golgi compartments to the lysosome (53).

In the yeast *Saccharomyces cerevisiae* most protein secretion also appears to occur via a constitutive default pathway (55). However, like mammalian lysosomal enzymes, proteins destined for the yeast vacuole depend on the presence of additional protein sorting information (21, 25, 56). The yeast vacuole is a prominent intracellular organelle which shares functional characteristics with both mammalian lysosomes and plant central vacuoles. This organelle is believed

1. *Abbreviations used in this paper*: Bb, Berkeley body; CPY, carboxypeptidase Y; ER, endoplasmic reticulum; FD, FITC-conjugated dextran; Inv, invertase; PrA, proteinase A; PrB, proteinase B.

to play an important role in the storage of amino acids and other small molecules (30). Like mammalian lysosomes, the yeast vacuole is an acidic compartment and contains a number of hydrolytic enzymes (33, 59). Certain of these hydrolases, including the glycoproteins proteinase A (PrA), proteinase B (PrB), and carboxypeptidase Y (CPY) have been shown to be synthesized at the level of the ER as inactive precursors. These proenzymes transit through the Golgi complex and are sorted to the vacuole, where they are processed to the mature active enzymes (16, 19, 32, 54). Sequence determinants have been defined within proCPY and proPrA that are necessary and sufficient to target these proteins to the vacuole (21, 25, 56). Mutational alterations in the proCPY sorting signal lead to missorting and secretion of the precursor form of this enzyme. Although the sorting signals in proCPY and proPrA lack any obvious primary sequence similarity, it is presumed that a common cellular protein-sorting apparatus mediates specific recognition and subsequent vacuolar localization of these enzymes. Each undergoes a similar set of compartment-specific modifications, and the kinetics for vacuolar delivery of both proteins are essentially the same (25). It seems likely that many soluble vacuolar proteins are segregated to this compartment via the same targeting mechanism.

In an effort to identify components of the vacuolar protein sorting apparatus, we recently isolated a number of mutants that exhibit defects in the proper localization and processing of several vacuolar proteins. These vacuolar protein targeting (*vpt*) mutants were identified using a gene fusion-based selection scheme. In wild-type cells, proCPY sequences fused to the gene for the normally secreted enzyme invertase (Inv) contain sufficient sorting information to divert delivery of enzymatically active Inv to the yeast vacuole (2, 21). Mutants have been selected that missort and secrete such CPY-Inv hybrid proteins. The ~600 mutants isolated thus far have been assigned to more than 33 complementation groups. The mutants exhibit hybrid protein-independent defects in the sorting of normal vacuolar enzymes including CPY, PrA, and PrB (46). Upon missorting, the precursor forms of these proteins are secreted, presumably because the selective vacuole protein delivery pathway is defective and the proteins then follow the default secretion pathway (2).

Given this large number of potential gene products that can influence the vacuolar protein-sorting process, it seemed likely that mutations in at least some of these genes might also affect biogenesis of a normal vacuole. Specifically, some of the proteins that are mislocalized in the *vpt* mutants may be essential in defining important structural and functional characteristics of this organelle. In addition, one might expect that lipid and protein constituents of the vacuole membrane would transit together with soluble vacuolar enzymes via a common vesicle carrier. Defects in vacuole membrane assembly therefore might also be expected in certain of the *vpt* mutants. To address these questions, we have assessed the vacuolar as well as other organellar morphologies in each of the *vpt* mutants. Using both light and electron microscopic techniques, we found that mutants in most of the *vpt* complementation groups still assembled morphologically normal vacuoles. However, mutants in three complementation groups accumulated what appeared to be multiple small vacuoles. Cells in four other *vpt* complementation groups exhibited extreme defects in vacuole biogenesis; these mutants accumulated vesicles and membrane-enclosed compartments that bore no resemblance to a normal vacuole. In addition, certain of the *vpt* mutants exhibited other phenotypes such as sensitivity to low pH or to osmotic stress. These observations provide insights into the mechanism(s) of vacuole biogenesis as well as the normal physiological role of this organelle.

Materials and Methods

Strains and Media

Mutants were isolated as described (46) from parental strains SEY6210 *MATα ura3-52 leu2-3,112 his3-Δ200 trp1-Δ901 lys2-801 suc2-Δ9* and SEY6211 *MATa ura3-52 leu2-3,112 his3-Δ200 trp1-Δ901 ade2-101 suc2-Δ9*. Other strains used were HMSF1 *MATα sec1-1* (37), SEY5078 *MATα sec7-1 suc2-Δ9 leu2-3,112 ura3-52* (this study), and SEY5186 *MATα* sec18-1 *leu2-3,112 ura3-52* (this study). Cells were grown on standard yeast extract peptone dextrose (YPD) or synthetic dextrose (SD) (synthetic minimal, supplemented as necessary) media (49). *ade2* strains were scored for the presence of red pigment after growth for 3–5 d on both standard YPD (containing 2% glucose) and YPD containing 8% glucose. Sensitivity to low pH was assessed on YPD adjusted to pH 3.5, 3.0, or 2.5 with 6 N HCl. Sensitivity to high osmotic pressure was determined on YPD containing 1.0 or 1.5 M NaCl, 1 M KCl, or 2.5 M glycerol (osmosity ~1.7s). As noted previously by Singh (51), certain batches of hypertonic media stored more than a few days inhibited growth of the wild-type strains; therefore it was important to test the media with a strain known to be resistant to the osmotic stress conditions present.

Genetic crosses, sporulation of diploids, and dissection of tetrads were performed as described by Sherman et al. (49).

Labeling of Cells with Fluorescent Dyes

All manipulations were performed at room temperature unless otherwise noted. Cells were labeled in the presence of FITC-dextran (FD) as described by Makarow (27), with the following modifications. Cells (5 ml) were grown in YPD to early log phase (1–2 × 10^7 cells/ml), centrifuged for 5 min in a clinical centrifuge (International Equipment Co., Needham Heights, MA), and washed once in YPD, pH 4.5. The cell pellet was resuspended to a concentration of 1.5 × 10^8 cells/ml in YPD, pH 4.5, containing 100 mg/ml 70 S FD, and incubated for 90 min at 37°C (or 25°C for temperature-sensitive (*ts*) strains) on a rotary shaker. The cells were centrifuged for 2 min at 6,000 rpm in a microcentrifuge (Savant Instruments Inc., Hicksville, NY), washed twice in PBS (10 mM Na-phosphate, pH 7.4, 140 mM NaCl), and resuspended in 0.4 ml PBS. The resuspended cells were mixed with low melting point agarose (0.5% final concentration) at 37°C, mounted on glass slides, covered with a coverslip which was sealed with nail polish, and observed immediately. Alternatively, cells were labeled with FITC as described previously (41). Cells (2 × 10^7) were resuspended in 1 ml YPD containing 50 mM Na-citrate, pH 5.5, and 10 μg/ml FITC in DMSO. After a 10-min incubation at 25°C with shaking, cells were centrifuged, washed once, and resuspended in 0.1 ml 100 mM K-phosphate, pH 7.5, containing 2% glucose. Cells were mounted as above.

For quinacrine labeling, cells were grown as described above and quinacrine was added to a final concentration of 175 μM in YPD, pH 7.6. After a 5-min incubation at 30°C, cells were centrifuged and mounted as above without washing. Ammonium acetate (200 μM final concentration) was added to the incubation mix where indicated (57).

For observation of the *ade2* endogenous fluorophore, cells were grown as described by Weisman et al. (57) and mounted as for FD.

Microscopy

Cells were observed using a Carl Zeiss Inc. microscope (Thornwood, NY), with a 100× oil-immersion objective, equipped for Nomarski optics and epifluorescence. Fluorescence filters used were Carl Zeiss Inc. BP450-490 (excitation), FT510 (beam splitter), and BP520-560 (emission barrier). All fluorescent images were photographed for 40–60 s using Eastman Kodak Co. (Rochester, NY) Tri-X Pan ASA400 film, increased to ASA1600 by using Diafine developer.

Electron Microscopy

Cells were prepared using a modification of the procedure of Byers and Goetsch (6). Cells (100 ml) were grown in synthetic minimal medium to an OD_{600} of ~0.3, shifted to YPD medium, and allowed to grow for one generation. The cells were harvested by centrifugation (5 min in an International Equipment Co. clinical centrifuge), washed in dH_2O, and fixed for 2 h at room temperature in 2 ml of 0.1 M Na-cacodylate, pH 6.8, 5 mM $CaCl_2$ (Buffer A), containing 3% gluteraldehyde. The fixed cells were washed once in 100 mM Tris-HCl, pH 8.0, 25 mM dithiothreitol, 5 mM Na_2-EDTA, 1.2 M sorbitol, and then incubated in the same buffer for 10 min at 30°C. To remove cell walls, the cells were centrifuged, washed once with 1 ml 0.1 M K-phosphate (adjusted to pH 5.8 with citric acid) containing 1.2 M sorbitol, and resuspended in 0.5 ml of the same buffer containing 0.05 ml β-glucuronidase type H-2 and 2.5 mg zymolyase. This cell suspension was incubated for 2 h at 30°C. The spheroplasts were centrifuged and washed in 1 ml buffer A. *ts* strains were shifted to 37°C for 3 h before harvesting and were fixed at 37°C for analysis at the nonpermissive temperature; the rest of the procedure was identical to that for non-*ts* strains. The reduced osmium-thiocarbohydrazide-reduced osmium membrane-enhancement staining technique was adapted from Willingham and Rutherford (60). Spheroplasts prepared as described above were resuspended in 0.5 ml 1% OsO_4, 1% K-ferrocyanide in buffer A, and incubated for 30 min at room temperature. After four washes in dH_2O (1 ml each), the cells were resuspended in 1% thiocarbohydrazide, incubated for 5 min at room temperature, and washed again four times in dH_2O. The cells were stained with 1% OsO_4, 1% K-ferrocyanide in buffer A for 3 min at room temperature, and washed in dH_2O as before. The samples were dehydrated through an ethanol series and embedded in London Ross White, which was allowed to polymerize for 3 d at 4°C with exposure to UV light. Thin sections were collected on 200-mesh copper grids, stained for 30–45 s with lead citrate (42), and observed on a transmission electron microscope (model 420; Philips Electronic Instruments, Inc., Mahwah, NJ).

Immunoprecipitations

Immunoprecipitations on labeled spheroplasts (46) were performed as described previously (25).

Materials

Bafilomycin A_1 was the generous gift of K. Altendorf, Universität Osnabrück, Osnabrück, FRG. Tran ^{35}S-label was purchased from ICN Radiochemicals, Irvine, CA. Gluteraldehyde, OsO_4, thiocarbohydrazide, and K-ferrocyanide were purchased from Polysciences, Inc., Warrington, PA. Zymolyase was purchased from Seikagaku Kogyo Co., Ltd., Japan, and low melting point agarose was purchased from Bethesda Research Laboratories, Gaithersburg, MD. Diafine developer was the product of Acufine, Chicago, IL. London Ross White embedding resin was purchased from Ted Pella Inc., Irvine, CA. FD (70 S), FITC, quinacrine, β-glucuronidase (type H-2), and all other chemicals not listed above were purchased from Sigma Chemical Co., St. Louis, MO.

Results

Vacuole Morphology in vpt Mutants

We have used light and fluorescence microscopy to determine the state of the vacuole in multiple *vpt* alleles from each of 33 complementation groups. In a wild-type strain grown in rich medium, yeast vacuoles occupy ~20% of the yeast cell volume and can often be visualized in the light microscope using Nomarski optics. However, small vacuoles can not be visualized by this technique and some cells do not appear to have any vacuole when observed by Nomarski optics (57). Therefore, in order to visualize even small vacuoles, we have taken advantage of a number of fluorescent dyes that specifically accumulate in this organelle.

FD as well as FITC[2] by itself have been used to label yeast vacuoles (27, 41). In wild-type cells, the vacuole appeared as a single large fluorescent spot or 2–3 spots of approximately equal size under the labeling conditions used (Fig. 1 *A*). A large vacuole was also visible in these cells using Nomarski optics. Unexpectedly, when the *vpt* mutants were examined using this dye, most of the mutants (26 complementation groups, see Table I) exhibited a vacuolar morphology indistinguishable from that of the parental strains (Fig. 1 *B*). We have grouped these mutants together and refer to them as class A *vpt* mutants. The remaining seven complementation groups exhibited an altered vacuolar morphology. In three of the groups (*vpt*3, 5, and 26), cells had multiple smaller organelles which were visible using Nomarksi optics and which stained with FITC (Fig. 1 *C*). This group of mutants has been designated class B. The remaining four *vpt* complementation groups (*vpt*11, 16, 18, and 33) had no intracellular structures which stained in the presence of FD. When observed by Nomarski optics, cells in these complementation groups appeared to have rough surfaces, and no vacuoles were visible (Fig. 1 *D*). We have defined this group of mutants as class C *vpt* mutants (Table I). These observations have been confirmed using two other fluorescent dyes that also accumulate in yeast vacuoles (see below).

Class A vpt Mutants Exhibit Wild-type Vacuole Morphology

We have studied the *vpt* mutants exhibiting each of the three vacuolar morphologies in more detail. In *ade*2 strains of *S. cerevisiae*, an endogenous fluorophore accumulates in the vacuole and can be visualized using fluorescence microscopy (57). By this method, the parental strains and the class A *vpt* mutants had vacuolar morphologies identical to those observed using FD (Fig. 1, *E* and *F*).

Like mammalian lysosomes (38), yeast vacuoles have an acidic pH (33) and can be labeled by dyes, such as quinacrine (1, 57), chloroquine (26), and neutral red (20, 34), which accumulate in a pH-dependent manner. These weak bases are presumed to diffuse through membranes and accumulate in acidic compartments (9). The vacuole morphology of wild-type cells as observed using quinacrine was identical to that seen with FD or the *ade*2 endogenous dye (Figs. 2 *A* and 4 *A*). Most of the class A *vpt* mutants also contained 1–3 large vacuoles which accumulated quinacrine, although in many cases the fluorescence was less intense than that in the parental strain (not shown). Multiple alleles of three complementation groups (*vpt*10, 13, and 24), exhibited very little or no vacuolar staining with quinacrine, although vacuoles were clearly visible by Nomarski optics in these cells (Fig. 2 *E*). These *vpt* mutants, which had morphologically normal vacuoles but exhibited no pH-dependent accumulation of dye, might carry mutations which affect vacuole acidification. In plant cells, the vacuole plays an important role in pH homeostasis; a decrease in external pH results in a lowered vacuolar pH, while the cytoplasmic pH remains constant (3). We reasoned that mutants defective in vacuole acidification might also exhibit defects in the regulation of intracellular pH. To address this issue, we tested whether any of the *vpt* mutants were sensitive to low pH. Growth was assayed on

2. While these studies were in progress, Preston et al. (41) reported that the vacuolar staining associated with FD was in fact due to nonendocytic uptake of FITC and other contaminating impurities in the FD. We have repeated the vacuole labeling experiments in a few of the *vpt* mutants using FITC and have observed vacuolar morphologies similar to those reported here for FD.

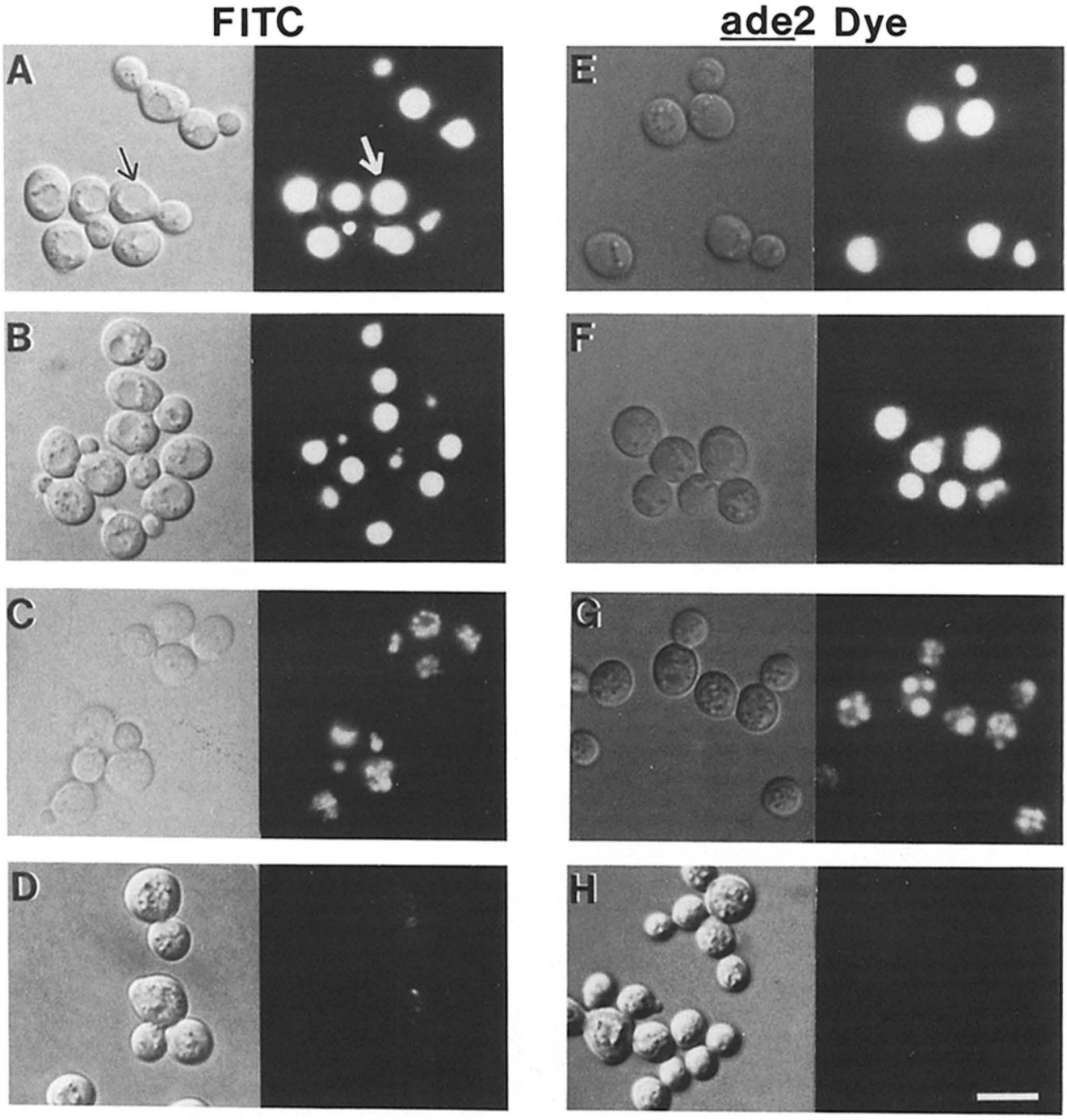

Figure 1. Vacuole morphology in *vpt* mutants labeled with FITC or the *ade2* endogenous fluorophore. (*A*, *B*, *C*, and *D*) Nomarski (left) and fluorescence (right) photomicrographs of cells labeled in the presence of FD (see Materials and Methods). (*E*, *F*, *G*, and *H*) Nomarski (left) and fluorescence (right) photomicrographs of cells grown in SD containing limiting adenine (12 μg/ml) to allow production of the *ade2* fluorophore. In each cell, the fluorescent spot corresponds to the vacuole, which appears as a large circular indentation using Nomarski optics (*arrows*). (*A* and *E*) Wild-type vacuole morphology as seen in the parental strains SEY6210 (*A*) or SEY6211 (*E*). (*B* and *F*) Representative class A *vpt* mutants, *vpt*10 (*B*) and *vpt*29 (*F*), in which the vacuole morphology is indistinguishable from that of the parent. (*C* and *G*) The class B *vpt* mutants, *vpt*5 (*C*) and *vpt*3 (*G*), contain multiple small vacuoles. (*D* and *H*) Representative class C *vpt* mutants, *vpt*18 (*D*) and *vpt*11 (*H*), which contain no structures that stain like vacuoles. Bar, 10 μm.

YPD media adjusted to pH 3.5, 3.0, or 2.5. The parental strains grew, although more slowly than on standard YPD, under these conditions. Strains in one complementation group, *vpt*13, were found to be extremely sensitive to low pH. Fourteen of 21 *vpt*13 alleles were unable to grow at pH 3.5, and 19 alleles of *vpt*13 were inhibited for growth at pH 3.0 (Fig. 3 *A*). Some alleles of other *vpt* mutants were also weakly sensitive to low pH (data not shown).

The existence of *vpt* mutants that exhibited possible defects in vacuole acidification led us to investigate the role of vacuo-

Table I. Summary of vpt Mutant Phenotypes

	Vacuole morphology	Abnormal growth phenotypes		Aberrant organelles accumulated
		Osmotic sensitive	Low pH sensitive	
Class A (*vpt*1, 2, 4, 6, 7, 8, 9, 10, 12, 13, 14, 15, 17, 19, 20, 21, 22, 23, 24, 25, 27, 28, 29, 30, 31, 32)	Wild-type vacuoles	*vpt*15, 29	*vpt*13	*vpt*15, 29-Bbs, vesicles *vpt*7, 28-"Golgi" *vpt*12-vesicles
Class B (*vpt*3, 5, 26)	Fragmented vacuoles	*vpt*26		
Class C (*vpt*11, 16, 18, 33)	No vacuoles	*vpt*11, 16, 18, 33		Multilamellar membrane structures, vesicles, Bbs

lar pH in the localization of proteins to the vacuole in wild-type cells. The vacuolar membrane contains a proton-translocating Mg^{++}-dependent ATPase which produces a proton gradient across the vacuolar membrane and acidifies the interior of the vacuole (24). The drug bafilomycin A_1 has been shown to be a specific inhibitor of the vacuolar membrane proton-translocating ATPase of *Neurospora crassa* (4). When wild-type yeast cells were treated with 10 μM bafilomycin A_1 for 10 min before staining with quinacrine, no vacuolar fluorescence was observed (Fig. 4 *B*). The inhibition of the pH-dependent quinacrine staining in these cells indicates that bafilomycin eliminates the pH gradient across the yeast vacuolar membrane, presumably by inhibiting the vacuolar membrane ATPase. To assess the role of the pH of the yeast vacuole in vacuolar protein localization, we next examined the effect of bafilomycin on the sorting and processing of vacuolar hydrolases. Spheroplasts were pretreated with bafilomycin (10 μM final concentration) for 10 min, radioactively labeled, and separated into intracellular and extracellular fractions before immunoprecipitation with CPY- and PrA-specific antisera. As shown in Fig. 4 *C*, in the absence of bafilomycin all of the CPY and PrA was processed to the mature enzyme form and remained associated with the yeast spheroplast fraction (0 μM, lanes *I* and *E*), indicating that these enzymes had been delivered to the vacuole (46, 59). In contrast, in the presence of bafilomycin, ~50% of the CPY was present in the proenzyme form, and most of this proCPY was secreted into the extracellular fraction (Fig. 4 *C*, 10 μM, lanes *I* and *E*). Bafilomycin caused a similar defect in the processing and targeting of PrA. Other agents known to raise vacuolar pH, including the weak base ammonium acetate (200–400 mM; reference 57) and the proton ionophore carbonyl cyanide *m*-chlorophenylhydrazone (CCCP; 40 μM) also caused the mislocalization of CPY and PrA (data not shown). Significantly, protein traffic to the cell surface was not disrupted under these conditions, and the concentration of bafilomycin used in these experiments did not inhibit yeast cell growth. Together these data indicate that vacuole pH plays a role in the efficient delivery and maturation of at least some vacuolar hydrolases.

We next examined the class A *vpt* mutants by transmission EM, using a technique that results in enhanced staining of biomembranes and structures containing glycomolecules (see Materials and Methods). As seen in Fig. 5 *A*, the vacuole stained as a large electron-dense compartment using this procedure. Thin sections of wild-type cells typically contained one large or two to three smaller vacuoles per cell. Other intracellular structures such as the nucleus, mitochondria, and ER were also readily visible. The majority of the class A *vpt* strains, such as the ones shown in Fig. 5, *B* and *C*, exhibited typical wild-type morphology. In thin sections of both wild-type and class A strains, we often observed an apparent substructure within the vacuole that did not stain like the rest of the vacuole and remained electron transparent (e.g., see Fig. 5 *B*). The significance of this structure is unclear, although it may represent the polyphosphate precipitate often observed in freeze-etched yeast cells (30).

Electron microscopic analysis also revealed that certain class A *vpt* mutants accumulated aberrant structures in addition to the normal vacuole. Mutants in two complementation groups, *vpt*15 and *vpt*29, contained organelles similar to those seen in yeast protein secretion (*sec*) mutants (37), including vesicles and Berkeley bodies (Bbs, structures presumably related to the Golgi complex; see reference 36). The electron micrographs in Fig. 6 show typical *vpt*15 and *vpt*29 cells and, for comparison, *sec*1 (accumulates vesicles), *sec*18 (accumulates ER), and *sec*7 (accumulates Bbs), prepared using the membrane-enhancement technique. The vacuoles in these *vpt*15 and *vpt*29 cells were abnormally large and occasionally contained inclusions (Fig. 6 *C*). This aberrant morphology was seen in every *vpt*15 and *vpt*29 allele examined. *vpt*13 and *vpt*26 cells also occasionally contained vesicles and Bbs (not shown).

In two complementation groups, *vpt*7 and *vpt*28, stacks of lamellae and reticular membrane arrays were observed at a high frequency (Fig. 7). These organelles were more prevalent in *vpt*7 and *vpt*28 than in the parental strain (i.e., 0.8–1.0 structure per cell section vs. 0.4 for the parent in 30–50 sections examined for each strain). These structures, which were usually not associated with any other organelle, are likely to correspond to exaggerated Golgi complexes. Finally cells in one class A mutant, *vpt*12, accumulated vesicles similar to those seen in the class C mutants (see below).

Class B vpt Mutants Exhibit an Altered Vacuole Morphology

Unlike the class A *vpt* mutants, cells in the three class B complementation groups (*vpt*3, 5, and 26) contained multiple compartments that stained in the presence of FD and were visible using Nomarski optics (Fig. 1 *C*). These small "vacuoles" also accumulated the *ade*2 endogenous fluorophore (Fig. 1 *G*). To determine whether these organelles had the lowered pH characteristic of wild-type vacuoles, we tested their ability to accumulate quinacrine. As shown in Fig. 2 *C*, the structures in the class B *vpt* mutants stained with quina-

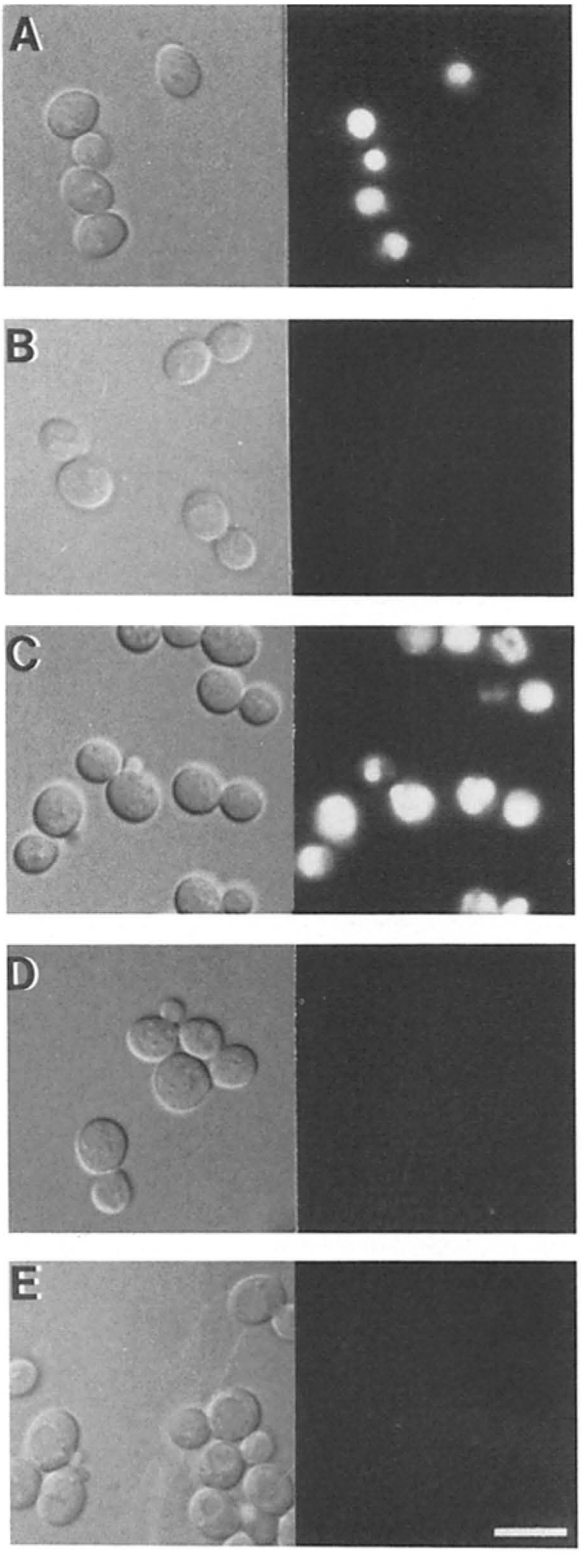

Figure 2. Quinacrine accumulation in the vacuoles of wild-type cells and *vpt* mutants. Cells were incubated in YPD, pH 7.6, containing 175 μM quinacrine for 5 min in the absence (*A*, *C*, and *E*) or presence (*B* and *D*) of 200 mM ammonium acetate. (*A* and *B*) Nomarski (left) and fluorescence (right) images of the parental strain SEY6210. (*C* and *D*) Nomarski (left) and fluorescence (right) images of *vpt5*, which exhibits a typical class B vacuole morphology. (*E*) *vpt13* exhibits no quinacrine staining (right), although vacuoles are clearly visible using Nomarski optics (left). Bar, 10 μm.

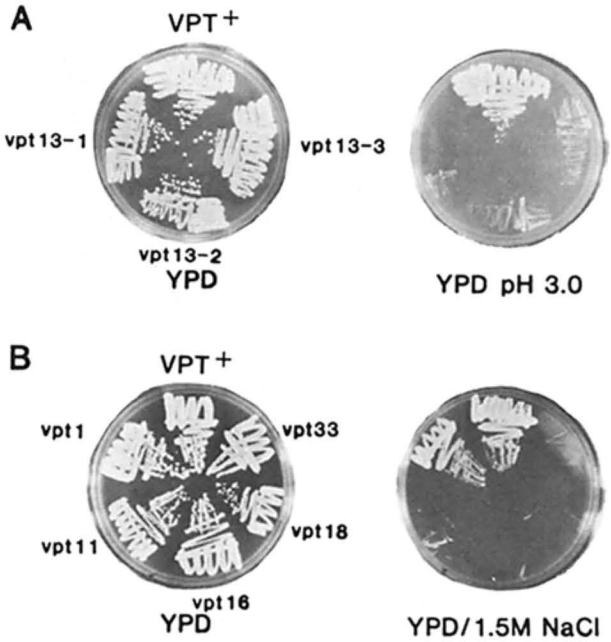

Figure 3. Growth defects associated with *vpt13* and the class C *vpt* mutants. (*A*) Three alleles of *vpt13* and the parental strain SEY6210 were streaked on YPD medium (left) or YPD medium adjusted to pH 3.0 with 6 N HCl (right). The plates were incubated at 30°C for 2 and 4 d, respectively. (*B*) A representative allele from each of the four class C *vpt* complementation groups was streaked on YPD medium (left) or YPD medium containing 1.5 M NaCl (right). The plates were incubated at 30°C for 2 and 5 d, respectively. The parental strain SEY6211 and a class A *vpt* mutant, *vpt1*, are shown for comparison.

crine, suggesting that these compartments had a pH similar to that of the vacuole in the parental strain. This hypothesis was further tested by labeling with quinacrine in the presence of ammonium acetate (57). Under these conditions, no fluorescent staining was observed in the parental strain or the class B *vpt* mutant (Fig. 2, *B* and *D*). This supports the hypothesis that the fluorescent staining observed in class B cells is due to the acidic pH of the compartments stained rather than to some nonspecific accumulation of dye.

The class B *vpt* mutants were also examined at the ultrastructural level to confirm the multiple-vacuole morphology observed by light and fluorescence microscopy. As seen in Fig. 5 *D*, a representative class B *vpt5* mutant allele contained multiple small organelles that stained like wild-type vacuoles. The number of vacuoles per cell section was quantitated for *vpt5* and for the parental strain (using 30–40 cell sections per strain). The average number of vacuole-like structures per cell section for the class B *vpt* was 5.7, while the number for the wild-type strain was 1.8. 71% of the class B cells, as compared to 16% of the parental cells, had 3 or more vacuoles. On the basis of the size of the vacuoles and the thickness of the sections, we have calculated that an average class B cell contains ~35 of these small vacuoles, while wild-type cells contain one to four vacuoles per cell. Representatives of the other two class B complementation groups (*vpt3* and *vpt26*) exhibited similar vacuolar morphologies when observed by EM.

Yeast which carry a mutation in the β-tubulin gene (*tub2*)

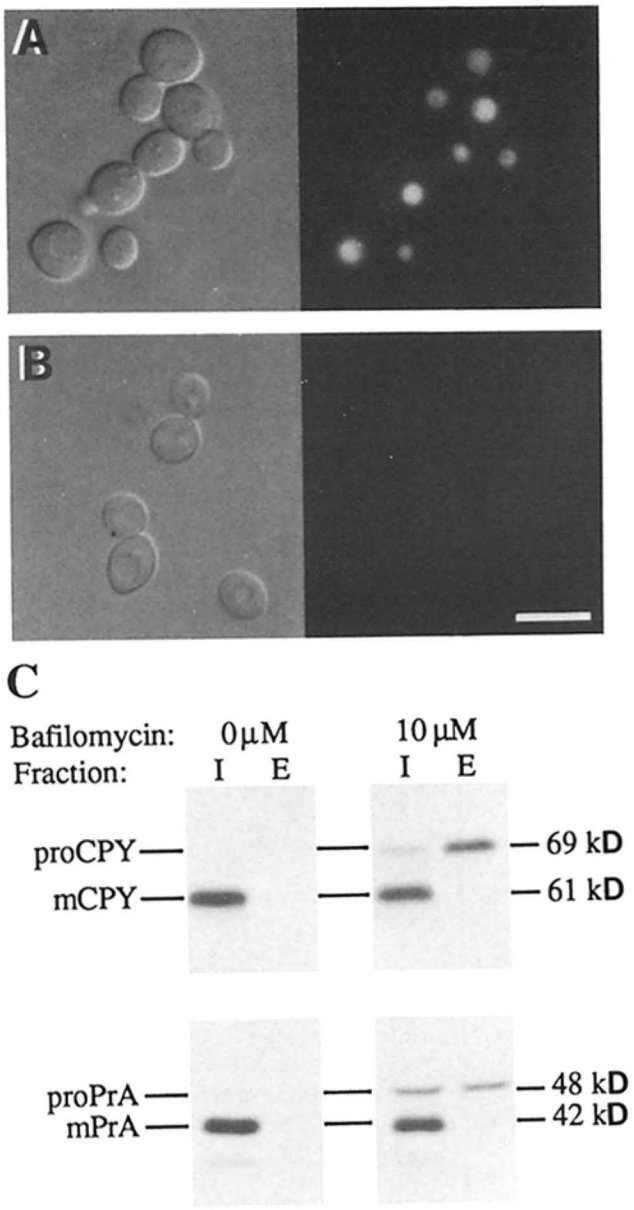

Figure 4. Effect of bafilomycin on vacuole staining with quinacrine and on vacuolar protein sorting. (*A* and *B*) Nomarski (left) and fluorescence (right) images of parental strain SEY6210 stained with quinacrine. Cells (2.5×10^7 in 0.25 ml) were preincubated for 10 min at 25°C in YPD, pH 7.6, in the absence (*A*) or presence (*B*) of 10 μM bafilomycin (in DMSO). An aliquot of cells (50 μl = 5×10^6 cells) from each sample was added to 400 μl of YPD, pH 7.6, containing 200 μM quinacrine without (*A*) or with (*B*) 10 μM bafilomycin. Cells were incubated for 5 min at 30°C, resuspended, and mounted as described in Materials and Methods. Bar, 10 μm. (*C*) Strain SEY6210 was enzymatically converted to spheroplasts as described (46). Bafilomycin was added to 10 μM final concentration as indicated 10 min before the addition of radioactive label. Cells were labeled with Tran ^{35}S-label for 20 min at 30°C and chased for 30 min by the addition of 5 mM methionine. Cultures were then separated into (*I*) intracellular (spheroplast) and (*E*) extracellular (periplasm and media) fractions (46). Immunoprecipitations with antisera to CPY and PrA were performed as described (25). The predicted locations and approximate molecular sizes of the different forms of CPY and PrA are indicated. Increased concentrations (100 μM) of bafilomycin did not increase the amount of missorted precursor CPY or PrA. Importantly, bafilmyocin had no effect on mitochondrial protein import (data not shown), which requires an electrochemical potential across the mitochondrial inner membrane (17).

or which have been treated with microtubule-disrupting drugs have a fragmented vacuole phenotype similar to that of the class B *vpt* mutants (15). We examined representative alleles of each complementation group by immunofluorescence, using anti-tubulin antibodies. No evidence of abnormal microtubule structures in any of the *vpt* mutants was observed (data not shown).

Class C vpt Mutants are Defective in Vacuole Assembly

Cells in four *vpt* complementation groups (*vpt*11, 16, 18, and 33) lacked any intracellular structures which stained in the presence of FD (Fig. 1 *D*). This phenotype was not simply due to an inability to sequester FITC in the vacuole; these mutants also failed to accumulate quinacrine or the *ade*2 endogenous fluorophore (Fig. 1 *H*). The *ade*2 dye is produced when a purine biosynthetic intermediate concentrates in the vacuole and undergoes oxidation and polymerization to produce a naturally fluorescent red pigment (23, 50). As a result, *ade*2 mutant yeast exhibit a red colony color when supplied with limiting amounts of adenine. All class A and B *ade*2 *vpt* mutants grown under conditions of limiting adenine were red. However, several *ade*2 alleles in each of the class C complementation groups were white. This phenotype was shown to be genetically linked to the *vpt* defect (see below). These observations suggest that in the absence of a functional vacuole, the purine biosynthetic intermediate is unable to undergo the reactions necessary to form the red color. We do not know whether the precursor accumulates in the cytoplasm or in other intracellular compartments, or whether it is secreted from the cell.

By EM, all class C mutants examined (at least two alleles of each of the four complementation groups) exhibited the same morphology (Fig. 8, *A–C*). Even at high magnification, these mutants appeared to lack any structure exhibiting the characteristic staining properties of a wild-type vacuole. Ultrastructural analysis also revealed that the class C *vpt* mutants accumulated a variety of novel membrane-enclosed organelles, including vesicles and Bbs. Fig. 8, *D* and *E* show higher magnification views of some of the structures that were exaggerated in these cells. The vesicles that accumulated in these mutants (Fig. 8 *D*) were enclosed by a membrane bilayer and were ~80 nm in diameter. In comparison, the vesicles that accumulate in the secretory mutant *sec*1 at nonpermissive temperature are ~100 nm in diameter and have a very different appearance from the vesicles seen in class C *vpt* mutants (37; see Fig. 6 *F*). As shown in Fig. 8 *E*, class C mutants also accumulated large, multilamellar, membrane-enclosed structures. Somewhat surprisingly, these structures were electron transparent, suggesting that they do not contain significant amounts of glycoproteins or sugars.

Several of the *vpt* complementation groups contain *ts* alleles (46). Four of these groups (*vpt*11, 16, 18, and 33) are class C, one (*vpt*3) is class B, and two (*vpt*15 and *vpt*29) are class A. These two class A mutants contained vacuoles but also accumulated organelles similar to those seen in the class C mutants (see above). We have examined the morphology

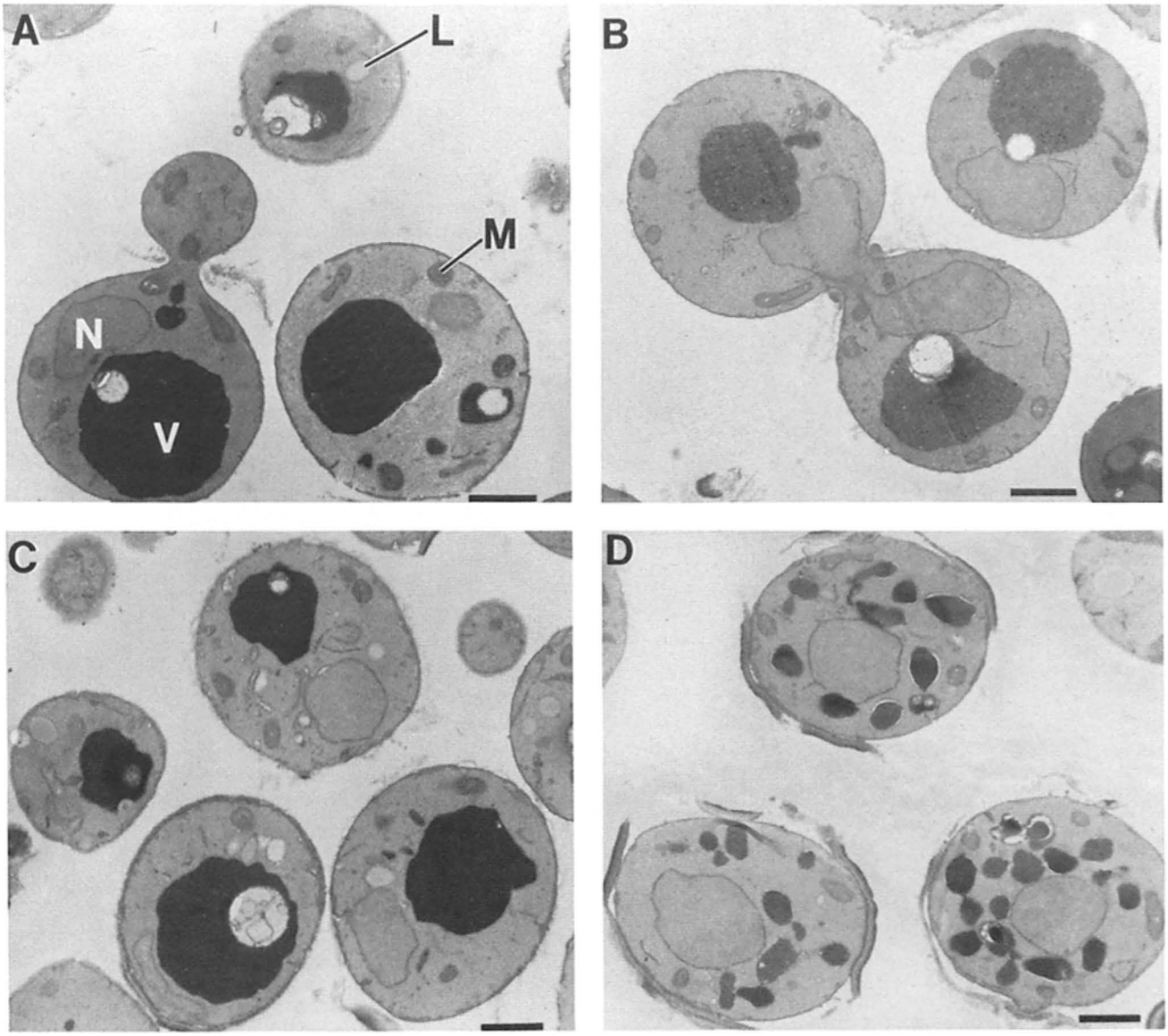

Figure 5. Electron micrographs of cells exhibiting wild-type, class A, and class B vacuole morphologies. Cells were prepared using the reduced osmium–thiocarbohydrazide-reduced osmium membrane-enhancement technique as described in Materials and Methods. (*A*) Parental strain SEY6210. Representative class A *vpt* mutants *vpt*17 (*B*) and *vpt*9 (*C*) also exhibit wild-type vacuolar and overall cellular morphology. *vpt*5 (*D*), a representative class B mutant, contains many small membrane-enclosed compartments which stain like wild-type vacuoles. *V*, vacuole; *N*, nucleus; *M*, mitochondrion; *L*, lipid droplet. Bars, 1 μm.

of these conditional lethal strains at both permissive (25°C) and nonpermissive (37°C) temperatures. Surprisingly, the vacuolar morphology of each of the *ts* strains examined was identical at 25°C and 37°C; aberrant organelles accumulated to the same extent at either temperature.

The existence of mutants in several complementation groups that lacked any apparent vacuole allowed us to begin to analyze the requirements for vacuole biogenesis in vivo. If a vacuole can be formed via a de novo synthetic pathway, diploids made by mating two class C mutants from different complementation groups should contain a normal vacuole. If, however, a preexisting normal template vacuole is necessary to direct the synthesis of the new organelle, diploids heterozygous for two class C mutations may be incapable of generating a vacuole despite the presence of both wild-type gene products. When we examined diploids made by crossing a *ts vpt*11 allele with a *ts vpt*18 allele, we observed that the diploid was temperature resistant, competent to sort vacuolar proteins, and contained a normal-appearing vacuole which stained with FITC. Homozygous diploids made by crossing two *ts* alleles of the same class C complementation group exhibited typical class C morphology and were *ts*, as expected. Furthermore, when the mating pairs were examined within 4–6 h of mixing, heterozygous class C zygotes were observed which clearly contained a vacuole in each of the conjugating cells, as well as in the diploid bud emerging from the zygote (Fig. 9). Ultrastructural analysis confirmed the presence of vacuoles in these heterozygous mating pairs

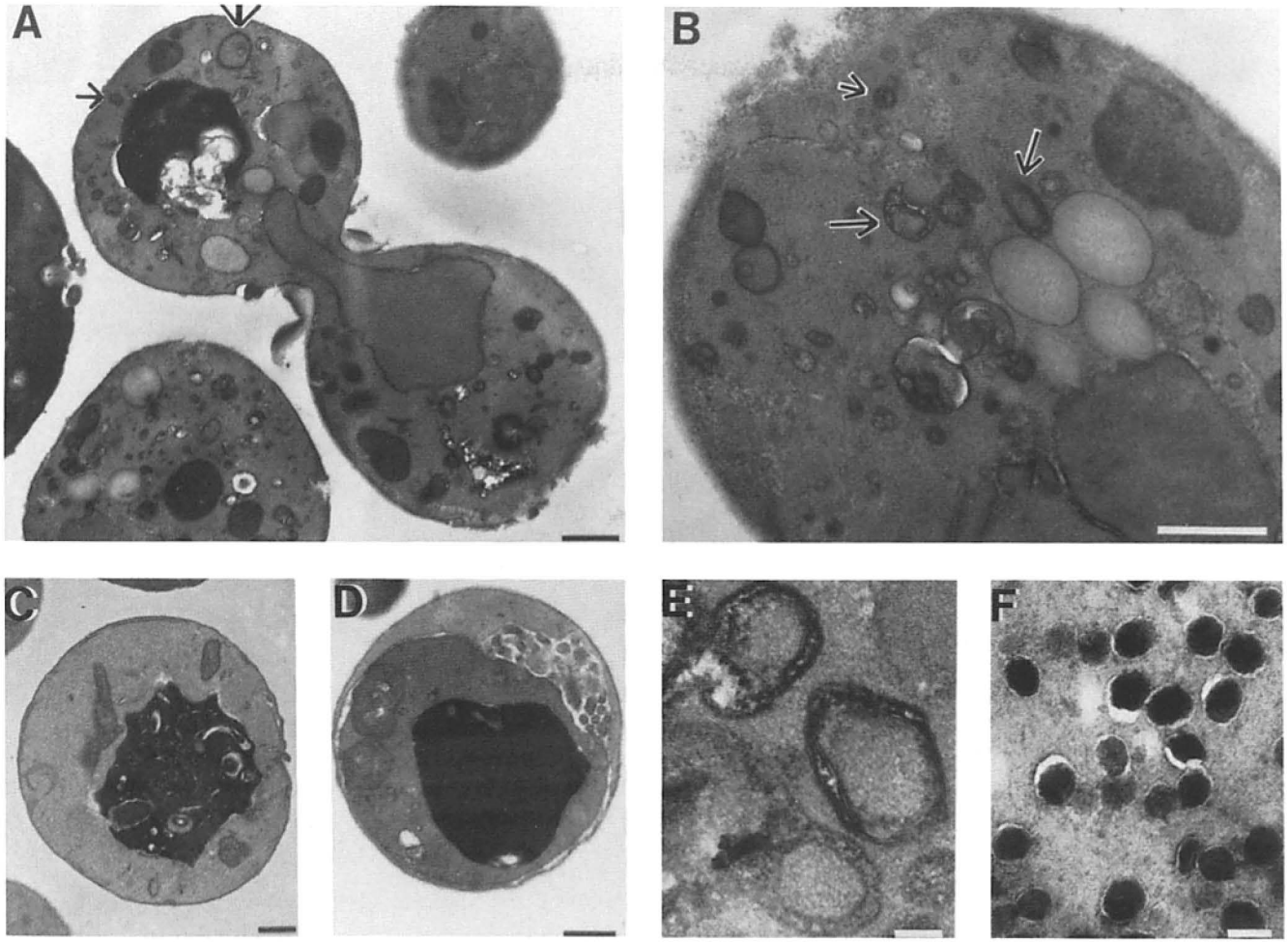

Figure 6. Electron micrographs of *vpt*15 and *vpt*29, class A mutants which exhibit aberrant organelles similar to those seen in certain of the *sec* mutants. Cells were prepared as described in the legend to Fig. 5. *vpt*15 (*A*) and *vpt*29 (*B*) cells contain Bbs (*large arrows*) and vesicles (*small arrows*) throughout the cytoplasm. (*C*) A typical *vpt*15 cell in which inclusions are seen in the vacuole. (*D*, *E*, and *F*) *sec* mutants (37) prepared using the membrane-enhancement technique, are shown for comparison. Each of the mutant strains was incubated at 37°C for 3 h before fixation. (*D*) Exaggerated tubular networks of membranes, presumably corresponding to ER, are clearly visible in this typical *sec*18 cell. (*E*) Accumulated Bbs are seen in this high magnification view of a portion of a representative *sec*7 cell. (*F*) A high magnification view of part of a *sec*1 cell shows an accumulation of secretory vesicles. These vesicles have a different appearance than those seen in *vpt*15 and *vpt*29 (compare with *A* and *B*). Bars: (*A*, *B*, *C*, and *D*) 0.5 μm; (*E* and *F*) 0.1 μm.

(not shown). These observations suggest that vacuole biogenesis can occur de novo in the absence of a normal template organelle. This assembly is rapid, occurring within one generation after conjugation. We cannot at present, however, exclude the possibility that the class C mutants contain tiny degenerate vacuole forms that are capable of functioning as templates or targets for new vacuolar protein and membrane delivery.

Class C Mutants are Defective in Several Vacuolar Functions

The vacuole has been implicated in a number of diverse cellular functions in wild-type cells, including osmoregulation (29), storage of amino acid reserves (30), endocytosis (43), and adaptation to adverse growth conditions (48). Like mammalian lysosomes and plant vacuoles (10, 28), the yeast vacuole may also mediate the normal intracellular turnover of macromolecules. Protein degradation increases dramatically during sporulation, and mutants lacking PrA or PrB activity are partially or completely defective in sporulation (22). We postulated that the class C *vpt* mutants, which exhibited extreme aberrations in vacuole assembly and morphology, might be defective in other cellular functions that may be vacuole related.

If the vacuole is required for adaptation to a change in external osmosity, one might expect that cells that lack a vacuole would be unable to survive in the presence of even a small increase in ionic or osmotic pressure. We assessed the growth of representative *vpt* alleles on YPD medium supplemented with 1.0 or 1.5 M NaCl, 1.0 M KCl, or 2.5 M glycerol. None of the class C mutants were able to survive, although the parental strains grew, under these conditions (Fig. 3 *B*). In addition, *vpt* 15, 26, and 29 were somewhat sensitive to the presence of 1.0 M NaCl or 2.5 M glycerol and were completely unable to grow on YPD medium containing 1.5 M NaCl. None of the other *vpt* mutants were sensitive to any of the osmotic stress conditions tested.

The class C mutants also exhibited other physiological

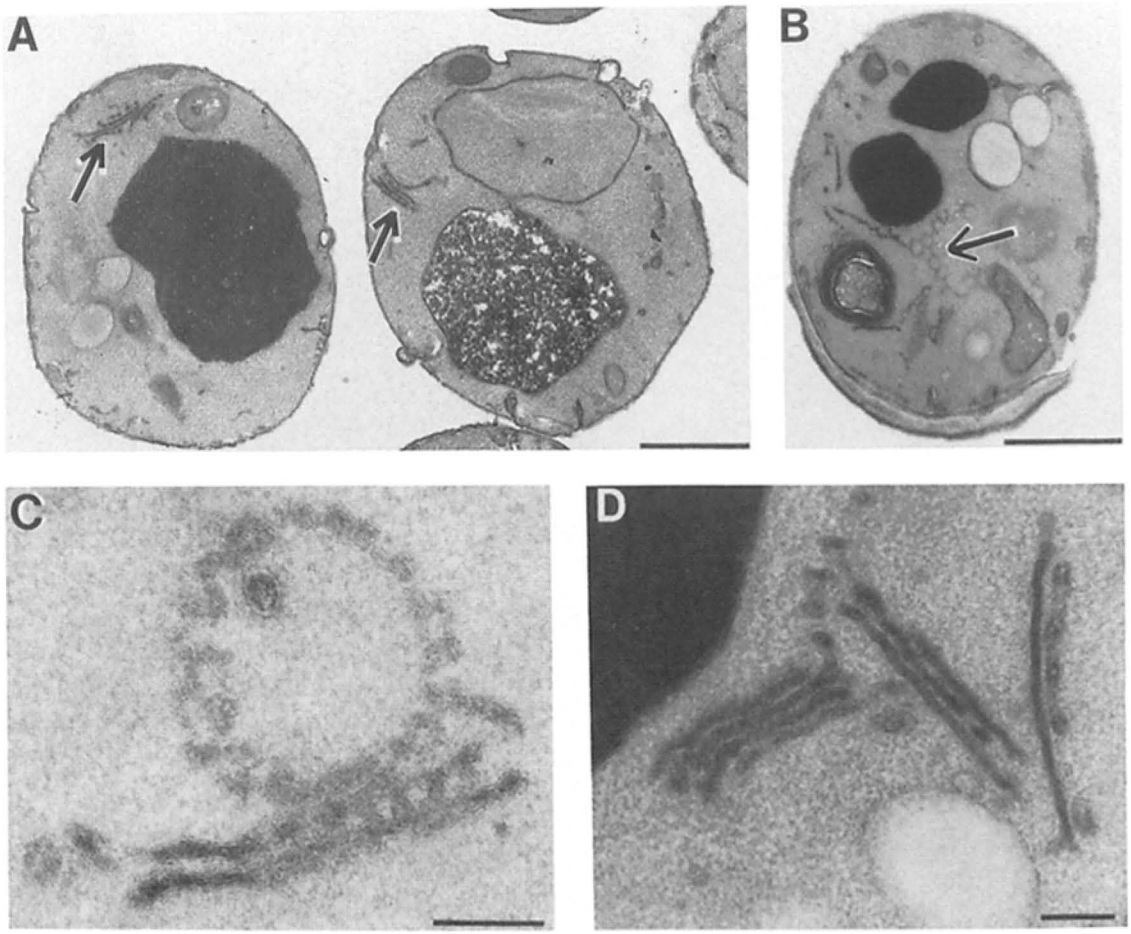

Figure 7. A gallery of electron micrographs of *vpt*28 and *vpt7*, which accumulate Golgi-like structures (*arrows*). Cells were prepared as described in the legend to Fig. 5. *A* shows *vpt7* cells; *B* shows a *vpt*28 cell. *C* and *D* are high magnification views of two Golgi-like structures representative of those seen in these mutants. Bars: (*A* and *B*) 1 μm; (*C* and *D*) 0.2 μm.

defects, including poor growth on nonfermentable carbon sources such as glycerol or lactate, poor growth in minimal media containing proline as the sole nitrogen source, poor sporulation of homozygous diploids, and low frequencies of DNA transformation. Furthermore, the class C *vpt* mutants contained smaller pools of basic amino acids than the class A or B *vpt* mutants, as judged by a filter assay for basic amino acids (reference 8; data not shown). Other cellular functions in the class C mutants, however, appeared to be normal. Based on the ultrastructural analysis, these mutants exhibited wild-type morphology of organelles such as the nuclei and mitochondria (see Fig. 8 *B*). The microtubules in these mutants appeared normal, as judged by immunofluorescence. Protein secretion also appeared to be unaffected in the class C as well as the other *vpt* mutants (46).

All vpt Phenotypes Cosegregate in Genetic Crosses

If the pleiotropic phenotypes discussed above all result from the *vpt* mutation in question, each of the phenotypes should cosegregate in genetic crosses of the mutants with wild-type cells. To confirm this, representative *vpt* mutants were backcrossed to the parental strain of the opposite mating type, the diploids were sporulated and tetrads were dissected. In this way, the vacuole morphology associated with each of the class B and class C *vpt* mutants was shown to cosegregate with the *vpt* defect (data not shown). The segregation of each of the other phenotypes associated with the class C mutants was also examined. In crosses between *ts* class C mutants and parental strains, all phenotypes showed the expected 2:2 segregation pattern. In each cross, the temperature sensitivity, osmotic sensitivity, and block in *ade*2 red pigment formation all cosegregated with the vacuole protein sorting defect. The results of a typical tetrad analysis for a *ts* class C mutant, *vpt*16, are shown in Fig. 10. Similar tetrad analyses also demonstrated that the low pH sensitivity exhibited by *vpt*13 cosegregated with the *vpt* sorting defect (data not shown).

Discussion

We have analyzed in detail the morphology and growth properties of a number of mutants defective in vacuole protein targeting. Three distinct vacuolar morphologies associated with the *vpt* mutants have been observed. The class A mutants, constituting 26 complementation groups, resembled the wild-type parent strains in that they had one or a few large vacuoles which were easily observed using light and fluorescence microscopy (Fig. 1, *A* and *B*). A second class of mutants,

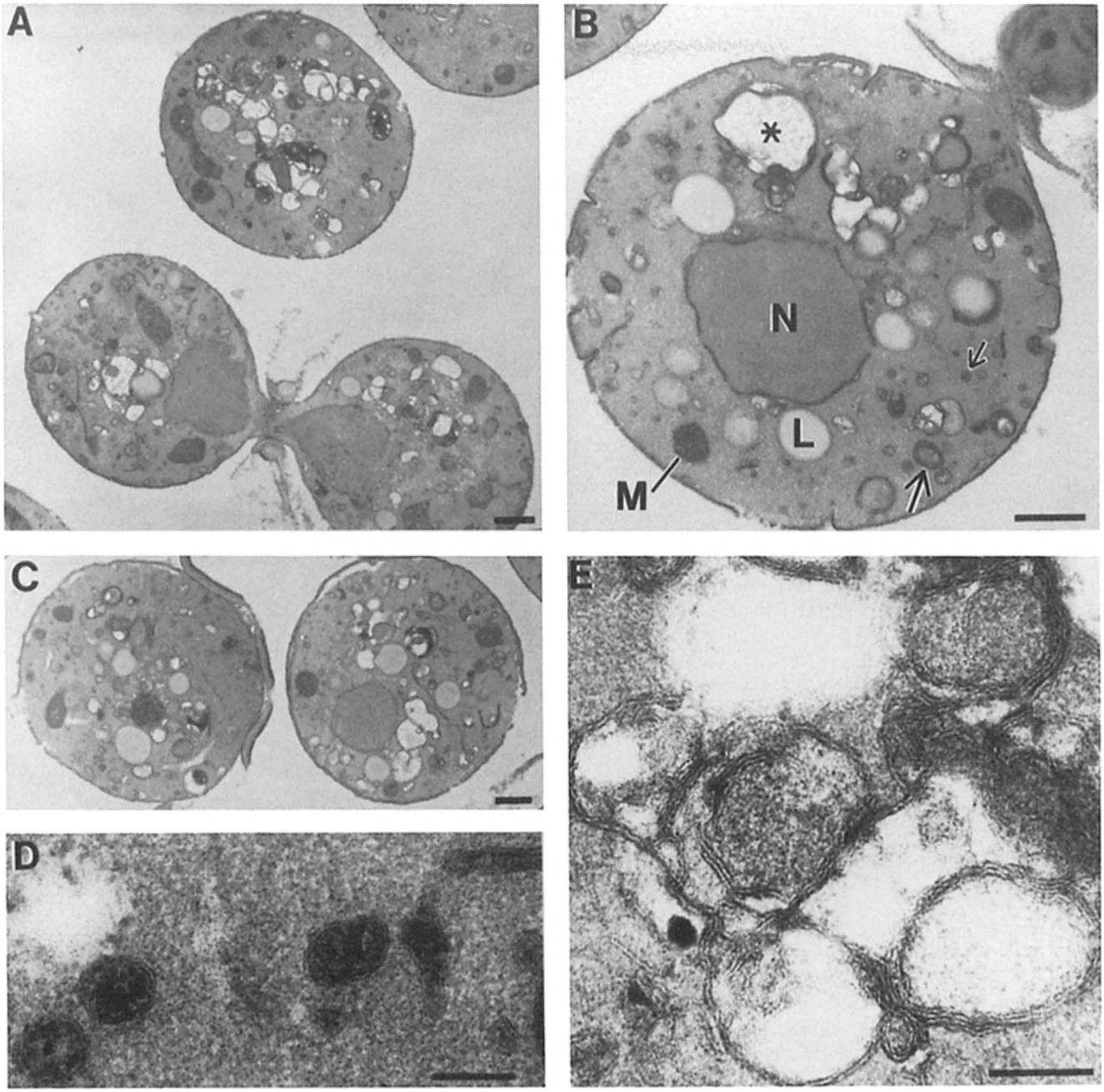

Figure 8. Electron micrographs of class C *vpt* mutants, which exhibit extreme defects in vacuole biogenesis. Cells were prepared as described in the legend to Fig. 5. (*A*, *B*, and *C*) Typical class C cells lack a discernible vacuole but accumulate aberrant organelles, including vesicles (*small arrow*), Bbs (*large arrow*), and large membranous structures (*asterisk*). *A* and *B* show *vpt*16 cells; *C* shows *vpt*11 cells. *D* shows a high magnification view of the vesicles that accumulate in class C cells (compare with vesicles in *sec*1 mutant, Fig. 6 *F*). *E* shows a high magnification view of the complex multilamellar arrays that accumulate in the cytoplasm in the class C *vpt* mutants. *N*, nucleus; *L*, lipid droplet; *M*, mitochondrion. Bars: (*A*, *B*, and *C*) 0.5 μm; (*D* and *E*) 0.1 μm.

class B, consisted of three complementation groups and was characterized by an altered morphology in which the vacuole was highly fragmented (Fig. 1 *C*). Mutants in the four class C complementation groups had no discernible vacuoles (Fig. 1 *D*), but accumulated small vesicles and other novel membrane-enclosed structures throughout the cytoplasm (Fig. 8).

The majority of the class A *vpt* mutants showed no apparent abnormalities in the vacuole itself or in other cellular features, as determined by electron microscopic analysis. In these mutants, at least some proteins presumably must continue to be properly targeted to the vacuole. Consistent with this idea, many of the class A *vpt* mutants mislocalize only a small fraction of CPY, PrA, PrB, or a CPY–Inv hybrid protein that contains vacuolar sorting information (46). It is possible that these mutants define functions which are only peripherally involved in vacuole protein targeting. However, other class A *vpt* mutants (*vpt* 1, 4, 6, 7, 15, 17, 29, and 30) exhibit gross defects in the localization and processing of

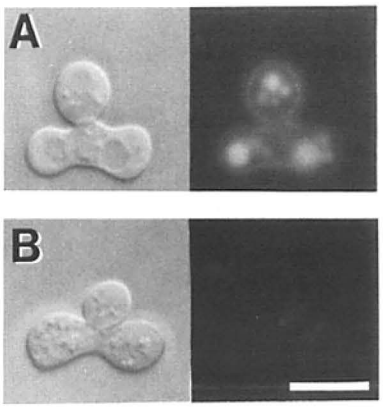

Figure 9. Heterozygous class C *vpt* zygotes form vacuoles within one generation after mating. (*A*) *vpt*18 (*MAT*α) and *vpt*33 (*MAT*a) cells were patched together on YPD medium and allowed to mate for 7 h at 25°C. Cells were scraped off the plate, resuspended in 1 ml YPD containing 50 μM Na-citrate, pH 5.5, and 1 μl of 10 mg/ml FITC was added. Cells were incubated for 10 min at 25°C, washed, and mounted as described in Materials and Methods. (*B*) Two *vpt*33 alleles were mated and stained as described in *A*. Bar, 10 μm.

vacuolar proteins, secreting as much as 70–100% of the CPY (46). These class A mutants still contain intact vacuoles and secrete <5% of the activity of a vacuolar membrane marker enzyme, α-mannosidase, suggesting that different pathways may exist for the sorting of soluble and membrane vacuolar proteins (see below).

Mutants in one of the class A complementation groups, *vpt* 13, exhibited extreme sensitivity to low pH (Fig. 3 *A*), suggesting that these cells may be unable to regulate their intracellular pH. The *vpt* 13 mutants were also defective in the pH-dependent accumulation of quinacrine in the vacuole (Fig. 2 *E*). In mammalian cells, endosomal acidity has been implicated in the proper localization of proteins to this organelle. Compounds such as amines that raise intralysosomal and endosomal pH (40) cause lysosomal enzymes to be secreted. The increase in pH appears to inhibit the uncoupling of lysosomal enzymes from their receptor carrier(s), resulting in a saturation of the available receptor sites (13). Furthermore, mammalian cell mutants have been described which appear to be defective in acidification of the endosome; these mutants secrete increased amounts of lysosomal hydrolases (45). In yeast, vacuolar pH may also play an important role in vacuole protein targeting. Treatment of wild-type yeast cells with ammonium acetate, the proton ionophore CCCP, or bafilomycin A_1, a drug which specifically inhibits the vacuolar ATPase, resulted in a block in the pH-dependent accumulation of quinacrine in the vacuole as well as the missorting of CPY and PrA (Fig. 4). Therefore, it seems likely that one or more of the *VPT* genes (e.g., *VPT*13) encode subunits of the vacuolar Mg^{++}-ATPase or other proteins involved in maintaining the vacuolar (or prevacuolar/endosomal) pH. Indeed, Stevens and colleagues (personal communication) have recently obtained data indicating that mutants in the *vpt* 13 complementation group exhibit levels of vacuolar ATPase activity that are tenfold lower than those in the wild-type strain.

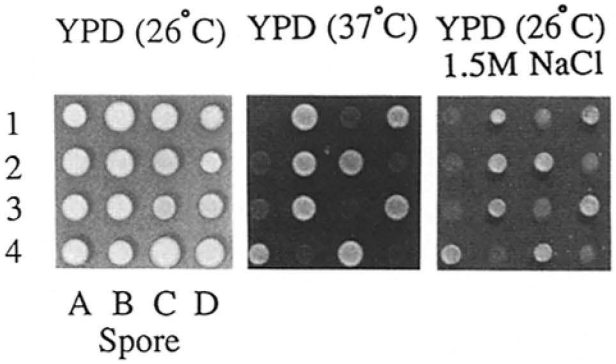

Figure 10. Cosegregation of the *ts* and osmotic-sensitive phenotypes in tetrads resulting from the sporulation of a *MAT*α *vpt*16/*MAT*a VPT+ diploid. *vpt*16 was crossed with parental strain SEY6211 and diploids were selected. Diploids were sporulated and tetrads dissected as described in reference 49. Segregants were patched onto YPD medium and replica-plated onto YPD medium which was incubated at 25°C or 37°C, or onto YPD medium containing 1.5 M NaCl (incubated at 25°C) as indicated. Segregants from four tetrads are shown. In each tetrad, the *ts* defect also was shown to be linked to the originally selected *vpt* phenotype, secretion of the CPY-Inv hybrid protein (46).

Unlike the class A *vpt*s, the class B mutants exhibited gross aberrations in vacuolar structure. The many small vacuole-like compartments observed in class B *vpt* mutants may represent the accumulation of an intermediate in vacuolar biogenesis or alternatively, fragmentation of a larger vacuole. These mutants might lack a vacuolar surface molecule which promotes fusion of small "prevacuolar" compartments to form a large vacuole. Alternatively, the gene products defined by the mutants could encode cellular constituents required to maintain the structural integrity of the organelle. These mutants also raise the issue of what exactly constitutes a vacuole. The organelles observed in the class B *vpt* mutants accumulated the dyes used to stain wild-type vacuoles and apparently had a similar acidic pH, as determined by the pH-dependent quinacrine staining (Fig. 2). However, the vacuole structures that accumulated in these mutants presumably are not recognized as valid destinations for certain vacuolar proteins, since the vast majority of PrA and CPY expressed in these mutants remains unprocessed and much is secreted (46).

The class C *vpt* mutants exhibited the most extreme defects in vacuole assembly among the *vpt* mutants isolated thus far. Many of these cells appeared to be essentially devoid of any organelles that resembled a vacuole, based on the criteria of size, shape, and histochemical-staining properties of normal vacuoles (Fig. 1 *D*). The observation that these cells are viable despite the absence of a vacuole indicates that many vacuolar functions may not be necessary under optimal growth conditions. Many of the class C mutants, however, are temperature sensitive for growth (46). The block in growth at 37°C exhibited by these mutants may indicate a requirement for a specific vacuolar function or, more likely, the cumulative effect of the loss of several vacuolar functions combined with the stress of growth at a temperature significantly above the preferred growth temperature of the organism.

The class C *vpt* mutants also exhibited an exaggeration of other organelles including Bbs, which are presumably related to Golgi structures and represent an intermediate com-

partment of the secretory pathway (36). The accumulation of Golgi-like structures or Bbs observed in these and certain other *vpt* mutants is consistent with a backup of vacuole proteins at the Golgi, the site of segregation for these proteins (54). In addition, the cytoplasm in these cells was filled with vesicles and complex lamellar arrays that might represent remnant vacuolar material or intermediates in vacuole biogenesis (Fig. 8). Several scenarios could account for the accumulation of organelles in these mutants. The gene products defined by the class C *vpt* mutants might correspond to essential components of a vacuolar protein sorting apparatus or to structural proteins of the vacuole itself. Alternatively, the class C *VPT* gene products might be involved in the regulation of organelle biogenesis, a process about which very little is known. Like its mammalian counterpart, the yeast vacuole may play an important role in the intracellular turnover of macromolecules. Perhaps in the class C mutants, organelles and membrane fragments accumulate because the cells lack a vacuole to perform this digestive function. The vesicles observed in these *vpt* mutants might represent intermediates in endocytic traffic that, in the absence of a vacuole, have no suitable target destination. On the other hand, the structures which accumulate in the class C mutants might represent actual intermediates in vacuole biogenesis. However, because these organelles are present at both permissive and nonpermissive growth temperatures, we are at present unable to test whether they correspond to actual reversible intermediates in the vacuole assembly pathway or are dead-end, nonreversible compartments. Additional experiments, such as immunoelectron microscopy or purification of the vesicles, will be required to address the nature of the content of these structures and their likely origin.

In plant cells, the large central vacuole plays an important role in regulating cell turgor pressure (3, 18, 61). Although not as extensively studied, it is possible that the vacuole may have a similar osmoregulatory function in yeast. High concentrations of solutes such as polyphosphates are stored in the yeast vacuole as osmotically inactive aggregates or polymers that could be converted into osmotically active forms by enzymatic digestion of the polymers. Large pools of sugars and basic amino acids (especially arginine) may also be present (29). Mutants in the four class C complementation groups were sensitive to osmotic stress (Fig. 3 *B*). Perhaps these cells are unable to accumulate the compounds normally used to generate high internal osmotic pressures. Alternatively, the osmotic-sensitive phenotype may not be directly related to vacuolar function. A number of seemingly diverse mutants, including nonsense suppressors, plasma membrane ATPase mutants, and actin mutants are sensitive to osmotic stress (31, 35, 51). Singh and Sherman (52) have suggested that, like *ts* mutations, alterations in a variety of essential proteins may make cells unusually sensitive to stressful growth conditions, in this case hypertonicity. Two class A *vpt* mutants (*vpt* 15 and 29) were partially inhibited for growth in the presence of hypertonic stress. The vacuoles in these strains were abnormally large and occasionally appeared to contain inclusions. Like class C *vpt* mutants, cells in these groups accumulated vesicles and Bbs (Fig. 6), and many of these strains are *ts* for growth. Furthermore, these mutants are severely defective in the processing and sorting of CPY and PrA (46). On the basis of the class C–like phenotypes exhibited by *vpt* 15 and 29, we propose that these mutants may represent an intermediate between the class A and C morphologies.

The class C *vpt* mutants are among the most defective in targeting CPY, PrA, and PrB to the vacuole (46). Unlike other *vpt* mutants, however, the class C mutants secrete 30–50% of the vacuolar membrane marker enzyme, α-mannosidase (46), indicating that the sorting defect in these mutants extends to membrane, as well as lumenal, proteins. Taken together, the data suggest that different recognition systems may participate in the sorting of soluble vacuole proteins, such as CPY and PrA, and vacuole membrane proteins (e.g., α-mannosidase). However, both sets of proteins may transit via common carrier vesicles or other intermediate compartments en route to the vacuole. According to such a model, the class C *vpt* mutants might affect protein sorting at the level of the common compartment. In contrast, the defects observed in many of the class A mutants, which mislocalize only a subset of the vacuole proteins, are likely to affect more specific components in the pathway, such as protein receptors.

A set of vacuolar protein localization (*vpl*) mutants similar to those described here has been isolated by selecting for the presence of active CPY in the periplasm (47). Some of these mutants also exhibit aberrant organelles such as Bbs and multivesicular bodies in addition to a normal vacuole. Complementation analysis has revealed that several of the *vpl* mutations fail to complement various *vpt* mutations. However, none of the *vpl* mutants exhibits the extreme defects in vacuole morphology seen in the class C *vpt* mutants (46, 47; Rothman, J., and T. Stevens, personal communication).

Two mutants which are defective in the accumulation of an endocytic marker, lucifer yellow carbohydrazide, and in pheromone response have been described by Chvatchko et al. (7). One of these mutants, *end* 1, has a morphology similar to that of the class C *vpt* mutants in that it lacks a vacuole and accumulates many small vesicles in the cytoplasm. This mutant is also defective in CPY processing (44) and sorting (46). Like the class C *vpt* mutants, *end* 1 grows poorly on glycerol (Dulic, V., and H. Riezman, personal communication) and is unable to grow under conditions of osmotic stress or high temperature. Crosses between *end* 1 and *vpt* 11 mutants have demonstrated that these two mutations define a single complementation group (46; Dulic, V., and H. Riezman, personal communication). This finding suggests that the vacuolar protein sorting and endocytic pathways may converge and that some gene functions may be common to both pathways. Geuze et al. have suggested that lysosomal enzymes are directed to the lysosome via a prelysosomal compartment which is also the site of uncoupling of endocytosed ligands and receptors (12). More recently, Griffiths et al. have identified a compartment in rat kidney cells which, by immunolocalization studies, appears to be shared by the lysosomal targeting and endocytic pathways (14).

The extreme defects in vacuole biogenesis, aberrations in vacuolar and cellular morphology, and increased sensitivity to suboptimal growth conditions observed in certain of the *vpt* mutants suggest strongly that vacuole structure and/or function are impaired in these strains. However, functions such as secretion and microtubule assembly appear to be normal in all of the *vpt* mutants (46). Although the class C *vpt* mutants, as well as *vpt* 15 and 29, accumulate organelles resembling those seen in certain *sec* mutants, complementa-

tion analysis has indicated that these *vpt* mutants and the *sec* mutants are not allelic (46). Other yeast mutations have been described which result in *vpt*-like morphological defects. A *ts* mutation in the single yeast actin gene (*act*1) leads to an accumulation of Bbs and vesicles similar to that seen in *vpt* 15 and 29 (35); however, complementation analysis indicates that none of the *ts vpt* mutants is allelic to *act* 1 (unpublished results). Likewise, although a deletion of the clathrin heavy chain gene in yeast causes severe morphological and growth defects, these cells continue to sort vacuolar proteins properly (39). A recently isolated mutant, *slp*1, exhibits a *vpt*-like morphology in that it lacks a central vacuole but contains many small vesicles throughout the cytoplasm (24a). We have not yet been able to test the allelism of this mutation with any of the *vpt* mutations.

The class B and C *vpt* mutants, which exhibit altered vacuolar morphologies, may define functions required for specific stages of vacuole biogenesis. These mutants may be especially useful for in vitro studies directed at reconstituting different steps in vacuole assembly. Molecular cloning of the *VPT* genes and characterization of the encoded gene products, coupled with the development of an in vitro system in which these gene products can be assayed, should help elucidate the roles these proteins play in vacuolar function, protein targeting, and organelle biogenesis.

We would like to thank Jean Edens for invaluable assistance with the electron microscopy, Michael W. Clark for the membrane-enhancement technique protocol and advice on the fluorescence microscopy, Paul Herman for helpful discussions and assistance with the zygote experiments, and John De Modena for technical assistance. We also thank K. Altendorf for the gift of bafilomycin A_1; Cathy Elkins for typing the manuscript; and Joel Rothman, Tom Stevens, Barry Bowman, and Howard Riezman for communicating their results before publication.

This study was supported by Public Health Service grant GM-32703 from the National Institutes of Health to S. D. Emr. L. M. Banta was supported by graduate fellowships from the National Science Foundation (NSF) and General Electric. J. S. Robinson was supported by graduate fellowships from the Evelyn Sharp Foundation, the Lucy Mason Clark fund, and the Markey Charitable Trust Fund. D. J. Klionsky was supported by a research fellowship from the Helen Hay Whitney Foundation. S. D. Emr is an NSF Presidential Young Investigator supported by NSF grant DCB-8451633.

Received for publication 26 May 1988, and in revised form 24 July 1988.

References

1. Allison, A. C., and M. R. Young. 1969. Vital staining and fluorescence microscopy of lysosomes. *Lysosomes Biol. Pathol.* 2:600–628.
2. Bankaitis, V. A., L. M. Johnson, and S. D. Emr. 1986. Isolation of yeast mutants defective in protein targeting to the vacuole. *Proc. Natl. Acad. Sci. USA.* 83:9075–9079.
3. Boller, T., and A. Wiemken. 1986. Dynamics of vacuolar compartmentation. *Annu. Rev. Plant Physiol.* 37:137–164.
4. Bowman, E. J., A. Siebers, and K. Altendorf. Bafilomycins: a new class of inhibitors of membrane ATPases from microorganisms, animal cells, and plant cells. *Proc. Natl. Acad. Sci. USA.* In press.
5. Burgess, T. L., and R. B. Kelly. 1987. Constitutive and regulated secretion of proteins. *Annu. Rev. Cell Biol.* 3:243–293.
6. Byers, B., and L. Goetsch. 1975. The behavior of spindles and spindle plaques in the cell cycle and conjugation of *Saccharomyces cerevisiae*. *J. Bacteriol.* 124:511–523.
7. Chvatchko, Y., I. Howald, and H. Riezman. 1986. Two yeast mutants defective in endocytosis are defective in pheromone response. *Cell.* 46: 355–364.
8. Cramer, C. L., and R. H. Davis. 1979. Screening for amino acid pool mutants of *Neurospora* and yeasts: replica-printing technique. *J. Bacteriol.* 137:1437–1438.
9. DeDuve, C., T. DeBarsy, B. Poole, A. Trouet, P. Tulkens, and F. van Hoof. 1974. Lysosomotropic agents. *Biochem. Pharmacol.* 23:2495–2531.
10. Ericsson, J. L. E. 1969. Mechanism of cellular autophagy. *Lysosomes Biol. Pathol.* 2:345–394.
11. Farquhar, M. G. 1985. Progression in unraveling pathways of Golgi traffic. *Annu. Rev. Cell Biol.* 1:447–488.
12. Geuze, H. J., J. W. Slot, G. J. A. M. Strous, A. Hasilik, and K. von Figura. 1985. Possible pathways for lysosomal enzyme delivery. *J. Cell Biol.* 101:2253–2262.
13. Gonzalez-Noriega, A., J. H. Grubb, V. Talkad, and W. S. Sly. 1980. Chloroquine inhibits lysosomal enzyme pinocytosis and enhances lysosomal enzyme secretion by impairing receptor recycling. *J. Cell Biol.* 85: 839–852.
14. Griffiths, G., B. Hoflack, K. Simons, I. Mellman, and S. Kornfeld. 1988. The mannose-6-phosphate receptor and the biogenesis of lysosomes. *Cell.* 52:329–341.
15. Guthrie, B., and W. Wickner. 1988. Yeast vacuoles fragment when microtubules are disrupted. *J. Cell Biol.* 107:115–120.
16. Hasilik, A., and W. Tanner. 1978. Biosynthesis of the vacuolar yeast glycoprotein carboxypeptidase Y. Conversion of precursor into the enzyme. *Eur. J. Biochem.* 85:599–608.
17. Hay, R., P. Böhni, and S. Gasser. 1984. How mitochondria import proteins. *Biochim. Biophys. Acta.* 779:65–87.
18. Hellebust, J. A. 1976. Osmoregulation. *Annu. Rev. Plant Physiol.* 27: 485–505.
19. Hemmings, B. A., G. S. Zubenko, A. Hasilik, and E. W. Jones. 1981. Mutant defective in processing of an enzyme located in the lysosome-like vacuole of *Saccharomyces cerevisiae*. *Proc. Natl. Acad. Sci. USA.* 78: 435–439.
20. Indge, K. J. 1968. The isolation and properties of the yeast cell vacuole. *J. Gen. Microbiol.* 51:441–446.
21. Johnson, L. M., V. A. Bankaitis, and S. D. Emr. 1987. Distinct sequence determinants direct intracellular sorting and modification of a yeast vacuolar protease. *Cell.* 48:875–885.
22. Jones, E. W. 1984. The synthesis and function of proteases in *Saccharomyces*: genetic approaches. *Annu. Rev. Genet.* 18:233–270.
23. Jones, E. W., and G. R. Fink. 1982. Regulation of amino acid and nucleotide biosynthesis in yeast. *In* The Molecular Biology of the Yeast *Saccharomyces cerevisiae*. Metabolism and Gene Expression. J. N. Strathern, E. W. Jones, and J. R. Broach, editors. Cold Spring Harbor Laboratory. Cold Spring Harbor, New York. 181–299.
24. Kakinuma, Y., Y. Ohsumi, and Y. Anraku. 1981. Properties of H^+-translocating adenosine triphosphatase in vacuolar membranes of *Saccharomyces cerevisiae*. *J. Biol. Chem.* 256:10859–10863.
24a. Kitamoto, K., K. Yoshizawa, Y. Ohsumi, and Y. Anraku. 1988. Mutants of *Saccharomyces cerevisiae* with defective vacuolar function. *J. Bacteriol.* 170:2687–2691.
25. Klionsky, D. J., L. M. Banta, and S. D. Emr. 1988. Intracellular sorting and processing of a yeast vacuolar hydrolase: the proteinase A propeptide contains vacuolar targeting information. *Mol. Cell. Biol.* 8:2105–2116.
26. Lenz, A.-G., and H. Holzer. 1984. Effects of chloroquine on proteolytic processes and energy metabolism in yeast. *Arch. Microbiol.* 137:104–108.
27. Makarow, M. 1985. Endocytosis in *Saccharomyces cerevisiae*: internalization of α-amylase and fluorescent dextran into cells. *EMBO (Eur. Mol. Biol. Organ.) J.* 4:1861–1866.
28. Matile, P. 1969. Plant lysosomes. *Lysosomes Biol. Pathol.* 1:406–430.
29. Matile, P. 1978. Biochemistry and function of vacuoles. *Annu. Rev. Plant Physiol.* 29:193–213.
30. Matile, P., H. Moor, and C. F. Robinow. 1969. Yeast cytology. *In* The Yeasts. A. H. Rose, and J. S. Harrison, editors. Academic Press, London. 219–302.
31. McCusker, J. H., D. S. Perlin, and J. E. Haber. 1987. Pleiotropic plasma membrane ATPase mutations of *Saccharomyces cerevisiae*. *Mol. Cell. Biol.* 7:4082–4088.
32. Mechler, B., M. Müller, H. Müller, M. Meussdoerffer, and D. H. Wolf. 1982. *In vivo* biosynthesis of the vacuolar proteinases A and B in the yeast *Saccharomyces cerevisiae*. *J. Biol. Chem.* 257:11203–11206.
33. Navon, G., R. G. Shulman, T. Yamane, T. R. Eccleshall, K.-B. Lam, J. J. Baronofsky, and J. Marmur. 1979. Phosphorus-31 nuclear magnetic resonance studies of wild-type and glycolytic pathway mutants of *Saccharomyces cerevisiae*. *Biochemistry.* 18:4487–4499.
34. Nishimura, M. 1982. pH in vacuoles isolated from castor bean endosperm. *Plant Physiol. (Bethesda).* 70:742–744.
35. Novick, P., and D. Botstein. 1985. Phenotypic analysis of temperature-sensitive yeast actin mutants. *Cell.* 40:405–416.
36. Novick, P., S. Ferro, and R. Schekman. 1981. Order of events in the yeast secretory pathway. *Cell.* 25:461–469.
37. Novick, P., C. Field, and R. Schekman. 1980. Identification of 23 complementation groups required for post-translational events in the yeast secretory pathway. *Cell.* 21:205–215.
38. Ohkuma, S., and B. Poole. 1978. Fluorescence probe measurement of the intralysosomal pH in living cells and the perturbation of pH by various agents. *Proc. Natl. Acad. Sci. USA.* 75:3327–3331.
39. Payne, G. S., T. B. Hasson, M. S. Hasson, and R. Schekman. 1987. Genetic and biochemical characterization of clathrin-deficient *Saccharomyces cerevisiae*. *Mol. Cell. Biol.* 7:3888–3898.

40. Poole, B., and S. Ohkuma. 1981. Effect of weak bases on the intralysosomal pH in mouse peritoneal macrophages. *J. Cell Biol.* 90:665–669.
41. Preston, R. A., R. F. Murphy, and E. W. Jones. 1987. Apparent endocytosis of fluorescein isothiocyanate–conjugated dextran by *Saccharomyces cerevisiae* reflects uptake of low molecular weight impurities, not dextran. *J. Cell Biol.* 105:1981–1987.
42. Reynolds, E. S. 1963. The use of lead citrate at high pH as an electron-opaque stain in electron microscopy. *J. Cell Biol.* 17:208–212.
43. Riezman, H. 1985. Endocytosis in yeast: several of the yeast secretory mutants are defective in endocytosis. *Cell.* 40:1001–1009.
44. Riezman, H., Y. Chvatchko, and V. Dulic. 1986. Endocytosis in yeast. *Trends Biochem. Sci.* 11:325–328.
45. Robbins, A. R., S. S. Peng, and J. L. Marshall. 1983. Mutant Chinese hamster ovary cells pleiotropically defective in receptor-mediated endocytosis. *J. Cell Biol.* 96:1064–1071.
46. Robinson, J. S., D. J. Klionsky, L. M. Banta, and S. D. Emr. Protein sorting in yeast: isolation of mutants defective in the processing and sorting of multiple vacuolar hydrolases. *Mol. Cell. Biol.* In press.
47. Rothman, J. H., and T. H. Stevens. 1986. Protein sorting in yeast: mutants defective in vacuole biogenesis mislocalize vacuolar proteins into the late secretory pathway. *Cell.* 47:1041–1051.
48. Schwencke, J. 1988. The vacuole, internal membranous systems and vesicles. *In* The Yeasts. A. H. Rose, and J. S. Harrison, editors. Academic Press, London. In Press.
49. Sherman, F., G. R. Fink, and C. W. Lawrence. 1979. Methods in Yeast Genetics: A Laboratory Manual. Cold Spring Harbor Laboratory, Cold Spring Harbor, New York. 1–98.
50. Silver, J. M., and N. R. Eaton. 1969. Functional blocks of the *ad*1 and *ad*2 mutants of *Saccharomyces cerevisiae*. *Biochem. Biophys. Res. Commun.* 34:301–305.
51. Singh, A. 1977. Nonsense suppressors of yeast cause osmotic-sensitive growth. *Proc. Natl. Acad. Sci. USA.* 74:305–309.
52. Singh, A., and F. Sherman. 1978. Deletions of the iso-1-cytochrome c and adjacent genes of yeast: discovery of the *osm*1 gene controlling osmotic sensitivity. *Genetics.* 89:653–665.
53. Sly, W. S., and H. D. Fischer. 1982. The phosphomannosyl recognition system for intracellular and intercellular transport of lysosomal enzymes. *J. Cell. Biochem.* 18:67–85.
54. Stevens, T., B. Esmon, and R. Schekman. 1982. Early stages in the yeast secretory pathway are required for transport of carboxypeptidase Y to the vacuole. *Cell.* 30:439–448.
55. Stevens, T. H., J. H. Rothman, G. S. Payne, and R. Schekman. 1986. Gene dosage-dependent secretion of yeast vacuolar carboxypeptidase Y. *J. Cell Biol.* 102:1551–1557.
56. Valls, L. A., C. P. Hunter, J. H. Rothman, and T. H. Stevens. 1987. Protein sorting in yeast: the localization determinant of yeast vacuolar carboxypeptidase Y resides in the propeptide. *Cell.* 48:887–897.
57. Weisman, L. S., R. Bacallao, and W. Wickner. 1987. Multiple methods of visualizing the yeast vacuole permit evaluation of its morphology and inheritance during the cell cycle. *J. Cell Biol.* 105:1539–1547.
58. Wieland, F. T., M. L. Gleason, T. A. Serafini, and J. E. Rothman. 1987. The rate of bulk flow from the endoplasmic reticulum to the cell surface. *Cell.* 50:289–300.
59. Wiemken, A., M. Schellenberg, and K. Urech. 1979. Vacuoles: the sole compartments of digestive enzymes in yeast (*Saccharomyces cerevisiae*)? *Arch. Microbiol.* 123:23–35.
60. Willingham, M. C., and A. V. Rutherford. 1984. The use of osmium-thiocarbohydrazide-osmium (OTO) and ferrocyanide-reduced osmium methods to enhance membrane contrast and preservation in cultured cells. *J. Histochem. Cytochem.* 32:455–460.
61. Zimmermann, U. 1978. Physics of turgor- and osmoregulation. *Annu. Rev. Plant Physiol.* 29:121–148.